# Generation of Raman solitons with minimal losses for dispersion radiation due to longitudinally nonuniform fiber

Dmitry A. Korobko, Andrei A. Fotiadi, Tigran A. Vartanyan, Igor O. Zolotovskii

Dmitry A. Korobko, Andrei A. Fotiadi, Tigran A. Vartanyan, Igor O. Zolotovskii, "Generation of Raman solitons with minimal losses for dispersion radiation due to longitudinally nonuniform fiber ," Proc. SPIE 11026, Nonlinear Optics and Applications XI, 1102613 (30 April 2019); doi: 10.1117/12.2520700

SPIE.

Event: SPIE Optics + Optoelectronics, 2019, Prague, Czech Republic

# Generation of Raman solitons with minimal losses for dispersion radiation due to longitudinally nonuniform fiber

Dmitry A. Korobko[a*], Andrei A.Fotiadi[a,b,c], Tigran A.Vartanyan[d], Igor O. Zolotovskii[a]

[a] Ulyanovsk State University, 432017, Ulyanovsk, Russia

[b]University of Mons, 31 Boulevard Dolez, B-7000 Mons, Belgium

[c] School of Engineering and Applied Science, Aston University, Birmingham, B4 7ET, UK

[d] Center of Information Optical Technologies ITMO University, Kronverkskiy pr. 49, 197101, St.Petersburg, Russia

## ABSTRACT

We report on numerical modeling of the spectral dynamics of telecom range laser pulse of moderate power in a silica fiber with a flattened dispersion and longitudinally varying diameter. In the simulation experiments, the optimal fiber profile has been proposed for more than 60% energy transfer from the initial telecom range pulse to subpicosecond pulse at 2.2-2.3 μm. Another option of the fiber diameter profile provides flat radiation spectrum in the range 2-2.5 μm.

**Keywords**: supercontinuum generation; dispersion varying fibers; Raman self-frequency shift.

## 1. INTRODUCTION

Due to a wide range of applications, design of supercontinuum laser sources is among hot topics of nonlinear fiber optics [1-3]. In this field, the current challenge is generation of a broadband spectrum in the visible and near-IR ranges. Supercontinuum sources operating at the wavelengths over 2 μm is of particular interest for applications in tomography, spectroscopy, and atmospheric analysis [4, 5]. To generate supercontinuum in this spectrum range special fibers, such as microstructured fibers based on oxide glass of complex composition [5] or fibers based on ZBLAN [6], are commonly used. However, poor compatibility of special fibers with the standard fiber laser sources makes this solution rather complicated. Supercontinuum generation above 2 μm in standard telecom silica fibers has been reported in Refs. [4, 7]. Alternative solution is the use of inhomogeneous fibers with the diameter varying along the fiber length. However, their applicability to this problem is still questionable.

The studies of supercontinuum generation in longitudinally inhomogeneous fibers performed since the 90s [8] for a long time have been limited to anomalous decreasing dispersion fibers used for generation of maximally broad and flat spectrum [1, 9-12]. Some interesting results have been obtained for laser pulse compression in increasing normal dispersion fibers [13]. However, modern drawing techniques allow fiber manufacturing with arbitrary longitudinal profiles of the dispersion (e.g., periodically fluctuating dispersion [14]). In fibers with a similar longitudinal profile, the supercontinuum generation scenario can be substantially extended. The known scenarios are generation of polychromatic dispersion radiation in a fiber of a special design with longitudinal profile of the zero dispersion wavelength (ZDW) synchronized with “red” Raman shift of a soliton pump pulse [15] or in a fiber with an axially oscillating profile allowing the generating soliton pulse to approach ZDW repeatedly [16]. So, the provided conditions lead to multiplication of the resonant radiation generation points along the fiber length and contribute to almost complete transfer of the pulse energy into a wide dispersion spectrum. In [17] an original way to control simultaneously the wavelength and duration of Raman-shifted solitons due to longitudinally non-uniform photonic crystal fibers was proposed. In [18] soliton pulse propagation is modeled in a tapered photonic crystal fiber for various taper profiles with the purpose of optimizing the

*korobkotam@rambler.ru

Nonlinear Optics and Applications XI, edited by Mario Bertolotti, Alexei M. Zheltikov, Proc. of SPIE
Vol. 11026, 1102613 · © 2019 SPIE · CCC code: 0277-786X/19/$18 · doi: 10.1117/12.2520700

Raman frequency shift. However, the interesting results of this work are limited to the case of a single fundamental soliton propagating in tapered fiber.

In this paper following the basic idea of [18], we continue to study the spectrum transformation of the pump pulse laying in the telecom range into the spectrum domain of 2 -2.5 μm employing fibers with different longitudinal dispersion profiles while maintaining a pulsed character of the radiation [19, 20].

## 2. THEORY AND NUMERICAL SIMULATIONS

Here, we study propagation of a laser pulse of moderate power injected into a fiber with an arbitrary variation of group velocity dispersion (GVD) along the fiber length and initially propagating in the anomalous dispersion domain. We limit our consideration to optical fibers with flattened dispersion. In such fibers, the third-order dispersion is low in absolute value and changes the sign. The fibers under consideration can be manufactured as a photonic crystal fiber with a broad fiber transmission spectrum ranging from 300 to 2500 nm or using a standard for telecom fibers pure silica preform with a W-profile of the refractive index, both with induced variations of the outer fiber diameter [21]. The fibers with a W-profile of the refractive index are used as prototypes for modeling in this paper. Fig. 1 presents the dispersion curves obtained for different values of fiber cladding diameter. Specifically, the anomalous dispersion spectral domain in these fibers is bounded by two ZDWs.

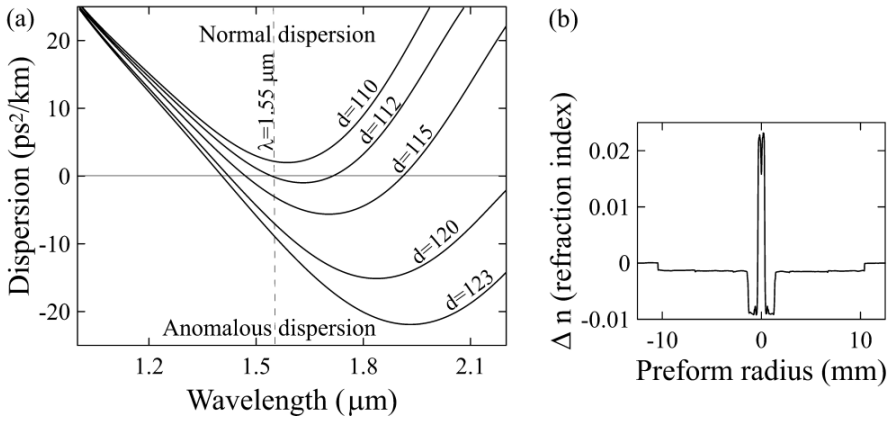


Figure 1. (a) Dispersion curves for fibers with flattened dispersion calculated for different values of the fiber cladding outer diameter (μm). (b) Refractive index profile of the fibers preform.

Numerical simulations of the pulse propagation along the optical fiber are based on the generalized nonlinear Schrödinger equation (NSE). The NSE describes the complex field amplitude $A(z,t)$ and takes into account high order dispersions (up to the 7th order $k \le 7$) and high nonlinear factors: stimulated Raman scattering and dispersion of nonlinearity [1]

$$\frac{\partial A}{\partial z} - \sum_{k\ge 2} \frac{i^{k+1}\beta_k(z)}{k!}\frac{\partial^k A}{\partial t^k} - \frac{lA}{2} = i\gamma\left(1+\frac{i}{\omega_0}\frac{\partial}{\partial t}\right)\left(A\int_{-\infty}^{\infty} R(t')\left|A(z,t-t')\right|^2 dt'\right) \quad (1)$$

Here, $\omega_0$ is the carrier frequency corresponding to the wavelength of $\lambda = 1.55$ μm,

$$R(t) = 0.82\cdot\delta(t) + 0.18\cdot\frac{\tau_1^2+\tau_2^2}{\tau_1\tau_2^2}\exp(-t/\tau_2)\sin(t/\tau_1)\Theta(t)$$

is the Raman response function, where the parameters $\tau_1 = 12.2$ fs, $\tau_2 = 32$ fs correspond to the silica fiber response, $\Theta(t)$ and $\delta(t)$ are the Heaviside and Delta functions, respectively. The dispersive parameters $\beta_k(z)$ ($\beta_2$ is the group velocity dispersion (GVD), $\beta_3$ is the third order dispersion, etc., $k \le 7$) are determined by the longitudinal profile of cladding diameter $d(z)$. Their values for the diameters presented in Fig.1 are obtained from polynomial approximation of dispersion curves and taken as the references (e.g., for $d = 115$ μm: $\beta_2 = -2.963\,\mathrm{ps^2km^{-1}}$, $\beta_3 = 0.04275\,\mathrm{ps^3km^{-1}}$, $\beta_4 = 1.882 \cdot 10^{-4}$ $\mathrm{ps^4km^{-1}}$, $\beta_5 = -2.69 \cdot 10^{-6}\,\mathrm{ps^5km^{-1}}$, $\beta_6 = 1.928 \cdot 10^{-8}$ $\mathrm{ps^6km^{-1}}$, $\beta_7 = -6.287 \cdot 10^{-11}\,\mathrm{ps^7km^{-1}}$). The intermediate values are calculated by second-order interpolation. The Kerr nonlinearity parameter $\gamma$ weakly depends on the outer cladding diameter and here is assumed to be unchangeable along the fiber length $\gamma = 6\ \mathrm{W^{-1}km^{-1}}$; $l$ is the loss in the fiber (0.25 dB/km).

Generation of resonant dispersive radiation is the physical effect accompanying the process of supercontinuum formation in optical fibers. The condition for generation of a low amplitude dispersive wave at the frequency $\omega_{DW}$ is the phase matching between the generating soliton and dispersive wave $\beta_s(\omega_{DW}) = \beta_{DW}(\omega_{DW})$, where $\beta_s$ and $\beta_{DW}$ are the propagation constants of soliton and dispersion waves, respectively. This condition can be expressed as [11, 15]:

$$\sum_{k\ge 2} \frac{\beta_k(\omega_0)}{k!}(\omega_{DW} - \omega_0)^k = \beta_{s0} + \beta_{s1}(\omega_s)(\omega_{DW} - \omega_s) + \frac{\gamma P}{2}, \qquad (2)$$

where $\beta_{s1}(\omega_s)$ is the inverted soliton group velocity at its frequency $\omega_s$, $P$ is the soliton peak power. Fig. 2 illustrates this relation for two cases: the soliton at the wavelength of $\lambda_S = 1.6$ μm and $\lambda_S = 1.75$ μm in the points corresponding to the fiber diameters of $d = 120$ μm and $d = 115$ μm, respectively. Assuming the pulse propagating in the fiber with a monotonically decreasing diameter (for simplicity, the peak power in both cases is $P = 500$ W) experiences a "red" Raman shift of the carrier wavelength from the initial value of $\lambda = 1.55$ μm. One can see that in the first case, the condition for generation of resonant dispersive radiation at the wavelength of $\lambda_{DW} \approx 1.2$ μm is satisfied. The radiation spectral intensity is

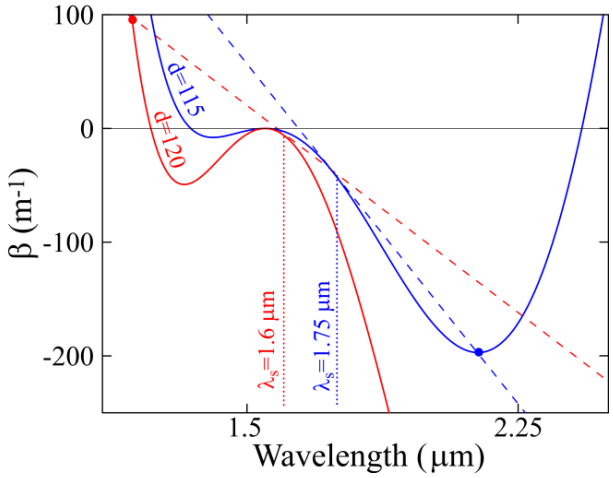


Figure 2. Scheme of dispersive wave generation by a soliton at different carrier wavelengths $\lambda_S$ in the fiber points of different diameters. $\beta_{DW}(\lambda)$ and $\beta_s(\lambda)$ are shown by solid and dashed curves. The domains of phase matching (2) are pointed by red and blue dots.

proportional to the soliton spectrum intensity at this frequency $\propto \mathrm{sech}^2\left(\pi\left(\omega_S-\omega_{DW}\right)\tau_S\right)$ [22] The second intersection outside the figure corresponds to generation of the radiation of negligibly low intensity, since the frequency difference is large. In the second case, generation of two resonance radiation domains at $\lambda_{DW}\approx 1.15$ μm (outside the figure) and with much higher intensity at $\lambda_{DW}\approx 2.2$ μm is also possible. As a result, it is expected that two spectral domains of resonant radiation with variable intensity and associated with two dispersion zero wavelength, (inflection points of the curves $\beta_{DW}(\lambda)$) are excited in the fiber with decreasing diameter as the pulse propagates through.

The aim of the work is to study the spectrum transformation associated with the telecom laser pulse propagation in an inhomogeneous fiber and to determinate the optimal longitudinal fiber profile $d(z)$ enabling high efficient energy transfer into the given spectrum range ( $\lambda > 2$ μm).

Let us determine the longitudinal profiles of optical fiber $d(z)$ that supports a shift of the soliton pulses formed through injection of an initial telecom range signal into the fiber towards the wavelength of $\lambda > 2$ μm and above due to stimulated Raman scattering and with minimal loss of the soliton energy. The dispersion in the range of soliton propagation is anomalous, obviously. The Raman self-shift velocity in a fiber with varying dispersion could be found from a well-known approximate relation between the velocity of Raman shift and the frequency [23] $d\Omega/dz \propto |D|/\tau^4$, where $\tau$ is the soliton duration, $D$ is the dispersion. For simplicity assuming an adiabatic manner of the soliton transformation and neglecting impact of high-order dispersions on soliton characteristics, i.e. maintaining the relation between the soliton energy and dispersion $|D|/\tau = \gamma E/2$, we can obtain

$$\frac{d\Omega}{dz} \propto \frac{\gamma E}{2}\frac{1}{\tau^3} = \frac{\gamma^4 E^4}{16\left|D(\omega_s, z)\right|^3}. \tag{3}$$

where $D(\omega_s, z) = \sum_{k\geq 2}\beta_k(z)\left(\omega_s-\omega_0\right)^{k-2}/\left(k-2\right)!$ is the local dispersion value (in $\mathrm{ps^2km^{-1}}$) taking into account not only the diameter changes but also displacement of the carrier frequency during the pulse propagation along the fiber (see Fig. 1).

Due to the dependence $d\Omega/dz \propto |D|^{-3}$, for getting a far Raman shift, it seems to be enough to inject a pulse into a fiber with low anomalous dispersion and then match the profile $d(z)$ providing the soliton Raman shift without an increase in the dispersion. So the longitudinal profile of tapered fiber with a flat dispersion dependence on the frequency can be obtained. Let us consider an example: a transform limited Gaussian pulse with a duration of $\tau_0 = 0.3$ ps and peak power of 250 W is injected into the fiber with the initial diameter of $d = 115.5$ μm (Fig. 3).

For the first 20 meters of the fiber, the diameter of $d(z) = 115.5$ μm is not changing and the anomalous GVD is $\beta_2 = -3.7\ \mathrm{ps^2km^{-1}}$. In this fiber section, the initial pulse breaks into a fundamental soliton with a maximum peak power that exhibits a "red" Raman shift and a residual radiation at the pump frequency. The residual pulse peak power is relatively low and its Raman shift is negligible. In this fiber segment, the soliton moving to the right crosses the dispersion curve minimum (see Fig. 1). After that, the fiber diameter increases synchronously with the fundamental soliton frequency $\omega_s$ to maintain the constant current fiber dispersion $D(\omega_s, z)$

To satisfy this condition, one should use a tapered fiber with a diameter increasing with the length in such a way that resonant radiation emission point shifts towards long wavelengths and center of soliton spectrum stays in a certain constant distance (~ 75 nm) from the second "red" zero dispersion ZDW 2 (Fig. 3). Due to this tapering, the soliton spectrum intensity in dispersion radiation emission point along the whole fiber length remains low, so transfer of soliton energy to the dispersive waves in the normal dispersion long-wavelength spectral domain (to the right of ZDW 2) is inefficient. The constant dispersion value at soliton carrier frequency maintains the constant spectrum width during the pulse propagation. The soliton peak power also tends to be approximately constant.

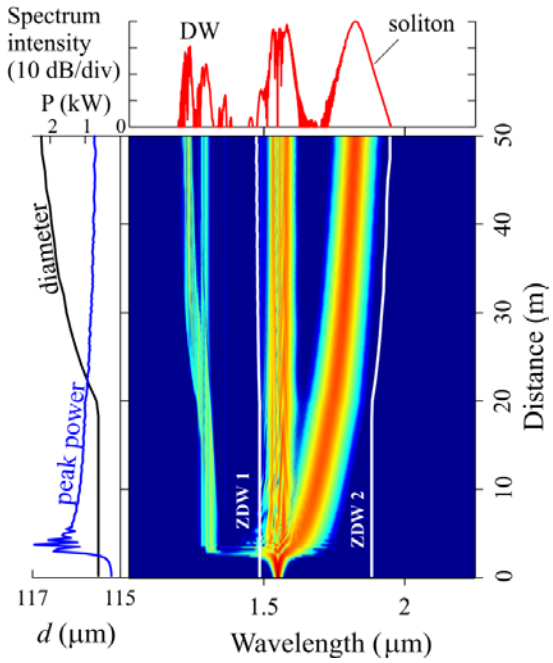


Fig. 3. Evolution of the pulse spectrum in an optical fiber with a diameter increasing with fiber length. Left: changes of the fiber diameter and radiation peak power along the fiber length. Top: radiation spectrum at the fiber output. DW is the dispersion radiation spectrum, ZDW 1 and ZDW 2 are changes of zero-dispersion wavelengths.

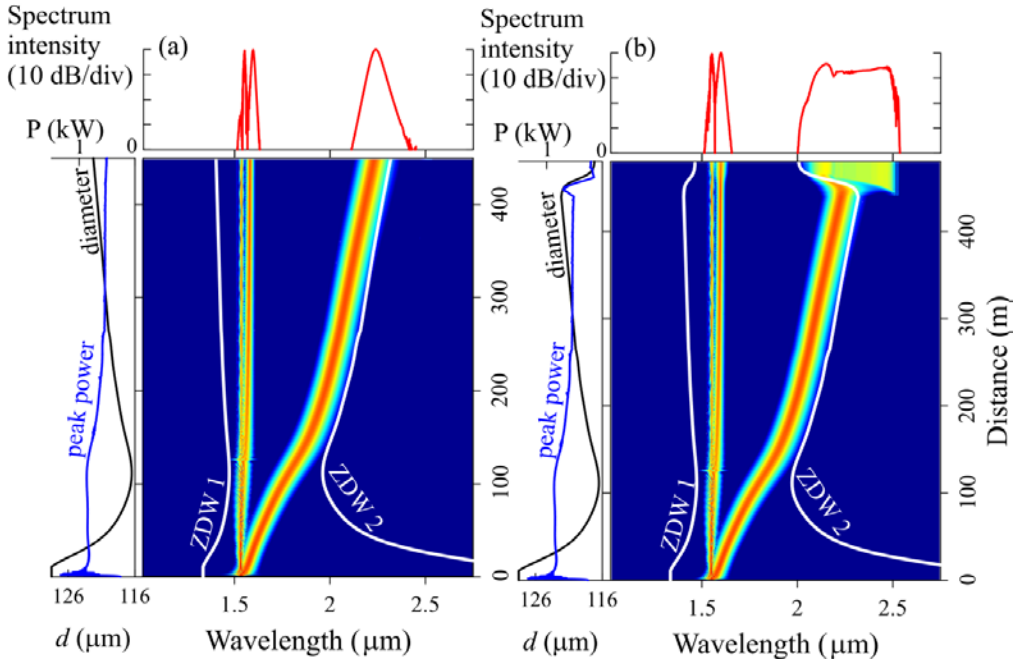


Figure 4. (a) Evolution of the initial pulse spectrum in an optical fiber with a special longitudinal profile. Left: change of the fiber diameter and radiation peak power along the length. Top: radiation spectrum at the fiber output. (b)The same as in fig. 4 (a), but diameter of the final fiber section (from 440 to 480 m) decreases rapidly.

However, low dispersion value in the first fiber section enhances generation of resonance dispersive radiation in the normal dispersion short-wavelength domain (to the left of ZDW 1). Even in the first fiber segment, when the compression of the input pulse occurs but the fundamental soliton is not formed yet, one can see the generation of dispersive radiation. Here, the higher peak power of the compressed pulse supports stronger energy transfer from the pulse. The Raman self-shift velocity also decreases due pulse energy loss (Eq.3). As a result, this technique does not allow to move a pulse to the wavelength over 2 μm using a fiber length of hundreds of meters. The resulting spectrum is a band of non-uniform intensity located in the range of 1.3-2 μm.

For efficient generation of pulses at a wavelength over 2 μm, we propose an alternative solution. In our configuration, the initial fiber section has a larger diameter and, consequently, higher anomalous dispersion, thereby allowing: 1) to avoid generation of short-wave resonant radiation at the initial stage; 2) to form a fundamental soliton of higher energy. The soliton order of the initial pulse is $N \propto |D|^{-1/2}$ [24], so, for a large initial dispersion a major part of the initial pulse energy belongs to the fundamental soliton. However, in this case, having passed the initial fiber segment with constant diameter, the soliton carrier wavelength occurs to the left of the dispersion curve minimum determined by the given initial diameter (Fig. 1). Then, the fiber diameter has to decrease to avoid an increase of the anomalous dispersion and decrease of the soliton peak power, and then, similar to the described case, the diameter has to increase in order to maintain a constant dispersion at the soliton carrier wavelength.

The spectrum evolution in this configuration is shown in Fig.4. Similar to the previous case, transform-limited Gaussian pulse with the duration of $\tau_0 = 0.3$ ps and peak power of 250 W is taken as an initial pulse. In the first fiber section with the length of 11m and $d(z) = 128.5$ μm ($\beta_2 \approx -17$ ps$^2$km$^{-1}$) a fundamental soliton separates from the initial pulse. Importantly, in this case, the resonance radiation is not generated. Then, in a 100 m fiber segment, the fiber diameter decreases. In this fiber section the profile of the diameter change maintains the soliton peak power constant during the Raman shift. (Note the small event at 120 m that is the second fundamental soliton of lower peak power and with much lower Raman shift rate separated from the pump. Further it will not be discussed). Importantly, the main soliton moving to "red" side goes beyond the frequency minimum of dispersion curve. Passing a short transition zone in the next segment, the fiber diameter smoothly increases ensuring a constant dispersion at the carrier wavelength.
Note, similar to the previous case, in this segment, the soliton peak power is nearly constant. As a result, at the output of 450 m fiber, a spectrum in the range of 2.2-2.3 μm contains more than 60% of full spectrum energy. Importantly, in contrast to a number of alternative converters [4-7, 25] transforming the pump pulse spectrum into a broadband supercontinuum comprising a dispersive component, in this case, the energy is concentrated above 2 μm and in a subpicosecond pulse with duration of about 120 fs and peak power of $P = 440$ W that is of interest for many applications. Besides, the optical fiber longitudinal profile can be designed to convert the output soliton pulse into spectrally flat dispersion radiation. For this, a fiber section several tens of meters long with a monotonically decreasing diameter could be attached to the described fiber configuration. The effect of ZDW shift rate on the characteristics of the dispersion wave spectrum generated by a soliton has been explained in Ref. [15]. At sufficiently slow approaching of the Raman shifted soliton to ZDW, the soliton detuning from the zero point GVD periodically increases and decreases, and therefore the intensity of the dispersion radiation is modulated in time. This modulation happens because the periodic recoil on the soliton from the intense radiation and new convergence of the soliton and the ZDW. Increasing the rate of the ZDW slope we can ensure that the ZDW moves fast enough so that it catches up not only with the bare shifted soliton but also with the addition from the recoil contribution. Then the latter does not adversely impact the radiation intensity as much, and the modulations smooth over, giving a homogeneous plateau in the spectrum and a strongly chirped radiation pulse in time domain. In this case, the spectrum is widened over shorter propagation distances, but the soliton crosses to the normal GVD spectral side, ending the radiation emission process. In the issue, the ZDW shift rate slightly affects the width but determines the flatness of the spectrum. In our case, the rate of the ZDW shift is fast enough for getting flat dispersion spectrum and suitable for the drawing technology based on fiber diameter change ($\sim 3\mu m / 10$ m ). The

performed simulation shows that the obtained subpicosecond pulse is converted into a flat spectrum radiation spread over a 2-2.5 μm range (fig 4 (b)).

A certain drawback of the proposed method is that a fiber with a special longitudinal profile is suitable for one type of initial pulse only. Numerical simulation demonstrates that the results shown in Fig. 4 are reproduced reasonably well for the same longitudinal fiber profile and an input Gaussian pulse with a peak power differing by not more than ± 0.7% from the given peak power and a wavelength differing by not more than ± 1 nm from 1.550 μm. For higher peak power or shorter wavelength, the earlier emission of the dispersion spectrum by a soliton occurs. As a result, at the fiber output, the subpicosecond pulse spectrum splits into 2 bands-the soliton (in the range around 2.1 μm or shorter) and the dispersion spectrum in the range of 2.3-2.4 μm. In the opposite case, (at lower peak power or longer wavelength), the Raman shift of the soliton stops earlier than expected and does not reach a range of 2.3-2.4 μm. However, even at not perfect matching of the parameters (about ± 5% for power and ± 5 nm for wavelength), the developed profile contributes to successful transformation of the spectrum of the pulsed telecom-range source into the wavelength region above 2 μm. This limitation does not allow the proposed approach to be applied universally. However, for a particular source with certain parameters of the output pulse one can calculate and simulate the longitudinal profile of the fiber that after drawing will be able to transform the spectrum as required. Of course, prediction of the practical applicability of the method can be done just after a series of experiments with various sources of subpicosecond pulses

## 3. CONCLUSION

We have considered the spectrum transformation of the pulse emitted by a laser operating in telecom spectrum range and moderate power as it propagates in an inhomogeneous silica fiber with a flattened dispersion. The performed computer simulation allowed us to find the optimal fiber profile providing transfer of more than 60% of the initial pulse energy to a subpicosecond pulse operating in the spectrum range of 2.2-2.3 μm. The resulting soliton pulse is spectrally isolated from other radiation and so can easily be filtered for further utilization with holmium or thulium amplifiers. In prospect, manufacturing of the fibers with the determined profiles will be followed by experimental verification of the proposed technique.


### Acknowledgments

The work was supported by the Russian Science Foundation (grant №18-12-00457), Russian Foundation for Basic Research (grant 18-42-732001 R-MK) and Russian Ministry of High Education and Sciences (State contract 3.3889.2017). A. A. Fotiadi acknowledges a support from the Leverhulme Trust (Visiting Professor, Grant ref: VP2-2016-042).


## REFERENCES


1. Supercontinuum Generation in Optical Fibers, ed. by J. M. Dudley and J. R. Taylor. (Cambridge University Press 2010).
2. G. P. Agrawal Nonlinear fiber optics: its history and recent progress, JOSA B. **28**(12) (2011) A1-A10.
3. A M. Zheltikov Let there be white light: supercontinuum generation by ultrashort laser pulses, Phys. Usp. **49** (2006) 605–628.
4. V A Kamynin, A S Kurkov, V B Tsvetkov, Supercontinuum generation in the range 1.6 — 2.4 μm using standard optical fibres, Quantum Electron. . 41 (11) (2011) 986–988.

5. R. Buczynski, H. T. Bookey, D. Pysz, R. Stepien, I. Kujawa, J. E. McCarthy & M. R. Taghizadeh, Supercontinuum generation up to 2.5 μm in photonic crystal fiber made of lead-bismuth-galate glass, Laser Phys. Lett. **7** (9) (2010) 666.
6. C. Xia, M. Kumar, O.P. Kulkarni, M. N. Islam, F.L. Terry Jr, M.J. Freeman & G. Mazé, Mid-infrared supercontinuum generation to 4.5 μm in ZBLAN fluoride fibers by nanosecond diode pumping, Opt. lett. **31**(17) (2006) 2553-2555.
7. A. S. Kurkov, E. M. Sholokhov, Y. E. Sadovnikova, All-fiber supercontinuum source in the range of 1550–2400 nm based on telecommunication multimode fiber, Laser Phys. Lett. **8**(8) (2011) 598.
8. K. Mori, H. Takara, S. Kawanishi, M. Saruwatari, T. Morioka, Flatly broadened supercontinuum spectrum generated in a dispersion decreasing fibre with convex dispersion profile, Electron. Lett. **33** (1997)1806–1808.
9. A. Kudlinski, A. K. George, J. C. Knight, J. C. Travers, A. B. Rulkov, S. V. Popov, & J. R. Taylor, Zero-dispersion wavelength decreasing photonic crystal fibers for ultraviolet-extended supercontinuum generation, Optics Express. 14(12) (2006) 5715-5722.
10. G. Genty, S. Coen, J. M. Dudley, Fiber supercontinuum sources, JOSA B. **24**(8) (2007) 1771-1785.
11. D. A. Korobko, O. G. Okhotnikov, D. A. Stoliarov, A. A.Sysolyatin, I. O Zolotovskii, Broadband infrared continuum generation in dispersion shifted tapered fiber, JOSA B. **32**(4), (2015) 692-700.
12. I. O. Zolotovskii, D. A. Korobko, O. G. Okhotnikov, D. A. Stolyarov & A. A. Sysolyatin, Generation of a broad IR spectrum and N-soliton compression in a longitudinally inhomogeneous dispersion-shifted fibre, Quant. Electron. 45(9), 844 (2015).
13. D. A. Korobko, O. G. Okhotnikov, D. A. Stoliarov, A. A. Sysoliatin, & I. O. Zolotovskii, Highly nonlinear dispersion increasing fiber for femtosecond pulse generation, Journ. Lightwave Tech. **33**(17) (2015) 3643-3648.
14. A. Mussot, M. Conforti, S. Trillo, F. Copie & A. Kudlinski "Modulation instability in dispersion oscillating fibers, Advances in Optics and Photonics. **10**(1), (2018) 1-42.
15. C. Milián, A. Ferrando and D. V. Skryabin, Polychromatic Cherenkov radiation and supercontinuum in tapered optical fibers, JOSA B. **29** (2012) 589–593.
16. A. Bendahmane, F. Braud, M. Conforti, B. Barviau, A. Mussot, A. Kudlinski, Dynamics of cascaded resonant radiations in a dispersion-varying optical fiber,. Optica. **1**(4) (2014) 243-249.
17. F. Braud, A. Bendahmane, A. Mussot, and A. Kudlinski, Simultaneous control of the wavelength and duration of Raman-shifting solitons using topographic photonic crystal fibers, JOSA B. **32** (2015) 2146-2152.
18. A. C. Judge, O. Bang, B. J. Eggleton, B. T. Kuhlmey, E. C. Mägi, R. Pant, & C. M.de Sterke, Optimization of the soliton self-frequency shift in a tapered photonic crystal fiber, JOSA B. 26(11) (2009) 2064-2071.
19. I. O. Zolotovskii, D. A. Korobko, V. Rastogi, D. A. Stoliarov, A. A. Sysolyatin, Subpicosecond pulse generation above 2 μm in longitudinally inhomogeneous single-mode fibres, Quantum Electron. 48(9) (2018) 813.
20. D. A. Korobko, V. Rastogi, D. A. Stoliarov, A. A. Sysolyatin, I. O. Zolotovskii, Generation of 2 μm radiation due to single-mode fibers with longitudinally varying diameter. Optical Fiber Technology. 47 (2019) 38-42.
21. U. G. Akhmetshin, V. A. Bogatyrev, A. K. Senatorov, A. A. Sysolyatin, & M. G. Shalygin, New single-mode fibres with the flat spectral dependence of the chromatic dispersion varying over the fibre length, Quant. Electron. 33(3) (2003) 265.
22. D. V. Skryabin, F.Luan, J. C. Knight, P. S. Russell, Soliton self-frequency shift cancellation in photonic crystal fibers, Science. **301** (2003) 1705–1708.
23. J. P. Gordon, Theory of the soliton self-frequency shift, Opt. Lett. **11** (1986) 662-664.
24. G. P Agrawal,"Applications of Nonlinear Fiber Optics" (Academic Press, San Diego, 2001).
25. V. A. Kamynin, A. S. Kurkov, V. M. Mashinsky, Supercontinuum generation up to 2.7 μm in the germanate-glass-core and silica-glass cladding fiber, Laser Phys. Lett. **9 (**3) (2012) 219.